

necessary changes were made in the upcoming models which were a bit developed than the existing models of that time but however these were limited to certain capabilities and needed a few changes which corresponds to the core objective of the proposed paper. Related works included automatic segmentation of the pericardium [11] They even considered thoracic cavity and combined region growing [8] with adaptive thresholds. However this alone wasn't sufficient and further models that addressed these issues were developed and this included the use of convolution neural network[16] which is a deep learning[15] method by which individual layers of the image was analyzed and mapped for better understanding of the image that was transmitted. This too was overcome with the proposal of a process referred to as segmentation[17] which was then combined with convolution neural network and was collectively referred to as ConvNets and segmentation[12] in which the network is provided as input with a patch in the centre and the process of analysis is done specifically to the pixels that lie next to the patches and in a similar way sever other patches are added for better analytical purposes. There was even an proposal on using fully convolutional networks (FCN) which was a variant of ConvNets but this too seemed inefficient against the system proposed. Though many such systems were proposed the need for development seemed to be on the rise with respect to the medical field and any further modification of the proposed system would benefit the society on the whole.

III METHODS

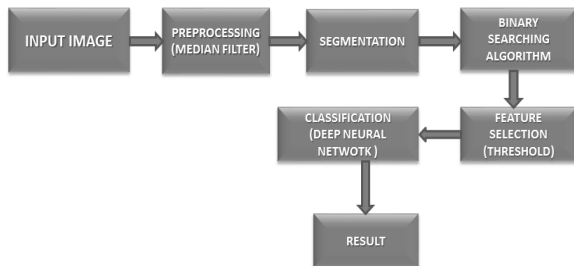


Fig 3.1: Workflow of the proposed system

A. Preprocessing

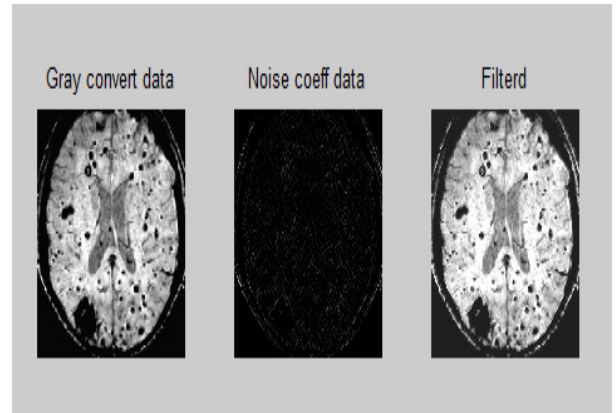


Fig 3.2:Pre-processing

The image pre-processing procedure is a very important step in the image processing. Colour processing is performed if the given input image is in colour. It is then converted into grey scale image. If the given input CT image is in grey scale, then pre-processing is performed without colour processing. The aim of the pre-processing phase is to obtain images which have normalized intensity, uniform size and shape. Finally, the images were scaled to the same size of 256×256 pixels.

B. Segmentation

The segmentation is carried out in multi-frame MRI in which the image is converted into discrete signals called samples where the number of samples are obtained by using the resolution formula $2^8(256 \text{ samples})$. The segmented 256 samples are analyzed and processed them further with feature extraction where the maximum pixel size and the minimum pixel size is identified along with the average pixel size. The individual samples are analyzed based on the abnormalities on the pixel size. K-means clustering is used to cluster the pixels into groups based on their intensities in order to separate the foreground pixels from the background pixels. Fuzzy C mean clustering is used to store the amplitude of the samples in an external fuzzy cluster memory which provides higher efficiency.

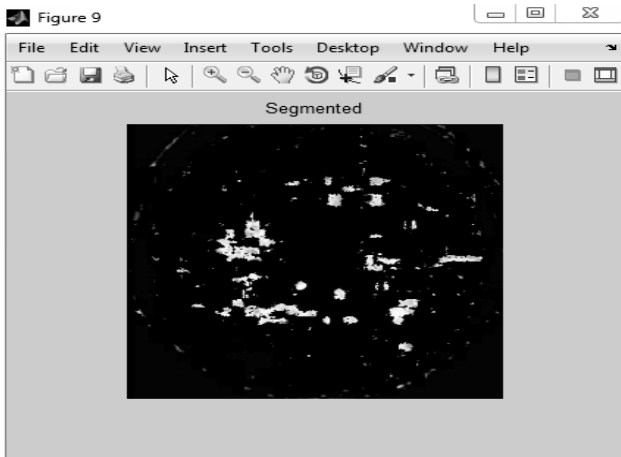


Fig.3.3: Segmentation

C. Feature extraction

The data given as input to an algorithm is too large to be processed so that the input data will be transformed into a reduced representation set of features (features vector). Feature Extraction is helpful in identifying brain tumour where is exactly located and helps in predicting next stage. It is a dimensionality reduction process, where an initial set of data is reduced to more manageable groups for processing, while still accurately and completely describing the original data set. The feature Extraction is achieved using Grey level co-occurrence matrix (GLCM) extraction. The features which are extracted from the CT image are Contrast, Correlation, Homogeneity, Entropy, Energy, Shape, Color, Texture and Intensity. The extracted features of the 256 samples are stored in Fuzzy cluster memory.

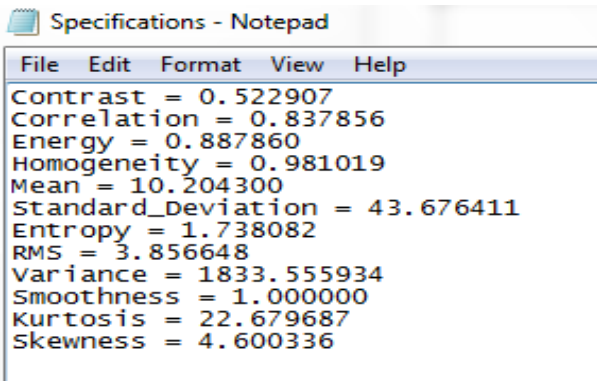


Fig 3.4: Specifications

D. Classification

RBFNN classifier is used for classification which is a combination of Fuzzy cluster, Artificial neural network

(ANN) and Radial basis function (RBF). The mapping properties of the RBFNN can be modified through the weights in the output layer, the centres of the RBFs, and spread parameter of the Gaussian function. The number of centres of RBF is fixed. If the number of centres is made equal to the number of input vectors of the exact RBF, then the error between the intended and actual network outputs for the training data set will be equal to zero. In this work, exact RBFNN was used due to its infinite range. The number of RBF centres was made equal to the number of input vectors. The feature set is classified using RBFNN classifier. Similarity matching was also performed by measuring the distance between vectors calculated for database images and query images.

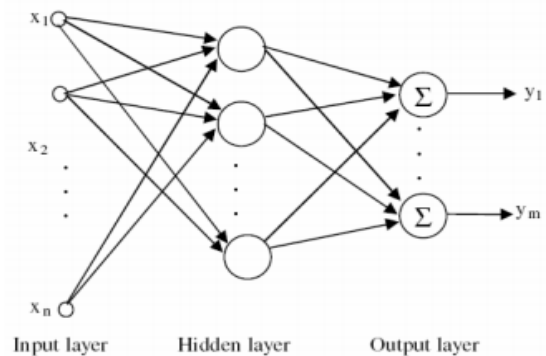


Fig. 3.5: Structure of Neural Network

IV EXECUTION AND RESULT

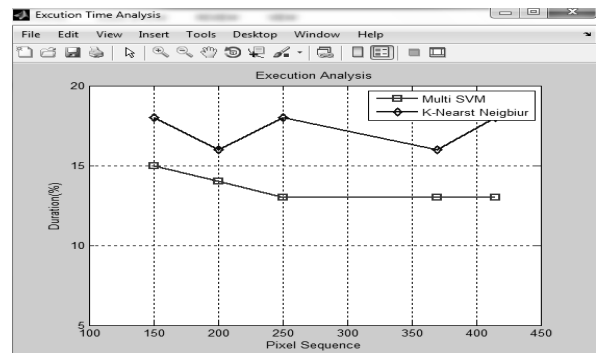


Fig 4.1: Execution Time

With the rise in the need for medical services around the globe the need for an mechanism that deals with the issues of a patient rather faster that the existing system was necessary which was the basic idea behind the development of such a beneficial outcome. And thus the result obtained was Highly accurate due to ANN. High sensitivity. And this process required Less amount of memory when compared to any of the previous models that are in existence today. Region based algorithm extracts the problematic area sharply thereby

enabling better understanding of the problem in hand. The epicardial and thoracic adipose tissue volumes from non-contrast CT datasets were focused which weren't so in the previous models and lacked the clear sense of understanding. The accuracy of proposed work using RBFNN based deep learning classifier increased the accuracy of the results with the help of RBFNN and CNN classifiers.

V CONCLUSION

A fuzzy logic based image segmentation approach is proposed for medical images comprising active contours and level set segmentation, to improve segmentation results. The pixels of level set segmentation are assigned weights, based on local entropy and local variance, evaluated by Fuzzy inference engine. Higher weights are assigned to pixels having less local entropy and less local variance, and vice versa. Simulation results of our proposed scheme have shown improvement in segmentation efficiency as compared with existing Convolution model. We propose and evaluate a new multi-task framework based on deep convolutional neural networks for fully automated quantification of epicardial and thoracic adipose tissue volumes from non-contrast CT datasets. The proposed method provided fast segmentation with strong agreement with expert manual volume measurements. The proposed approach may represent a tool for rapid measurement of EAT volume as an imaging biomarker for future clinical use, offering promise for improved prediction of adverse cardiac events. As a result, large reduction of the processing units and great improvement of the algorithm anti-interference make the algorithm improve not merely convergence speed but also segmentation accuracy. Besides, the practical application of K-means clustering segmentation algorithm is greatly improved in 3D medical data field segmentation.

REFERENCES

- [1] Frederic Commandeur, Markus Goeller, Julian Betancur, Sebastien Cadet, Mhairi Doris, Xi Chen, Daniel S. Berman, Piotr J. Slomka, Balaji K. Tamarappoo, Damini Dey "Deep Learning for Quantification of Epicardial and Thoracic Adipose Tissue from Non-Contrast CT", *IEEE Transactions on Medical Imaging, TMI*. 2018. 2804799, 2009.
- [2] M. Shimabukuro, Y. Hirata, M. Tabata, M. Dagvasumberel, H. Sato, H. Kurobe, D. Fukuda, T. Soeki, T. Kitagawa, S. Takanashi et al., "Epicardial adipose tissue volume and adipocytokine imbalance are strongly linked to human coronary atherosclerosis," (in eng), *Arterioscler Thromb Vasc Biol*, vol. 33, no. 5, pp. 1077-84, May 2013.
- [3] T. Mazurek, L. Zhang, A. Zalewski, J. D. Mannion, J. T. Diehl, H. Arafat, L. Sarov-Blat, S. O'Brien, E. A. Keiper, A. G. Johnson et al., "Human Epicardial Adipose Tissue Is a Source of Inflammatory Mediators," *Circulation*, vol. 108, pp. 2460-2466, 2003.
- [4] V. Y. Cheng, Dey, D., Tamarappoo, B.K., Nakazato R, Gransar, H, Miranda-Peats R, Ramesh A, Wong N.D., Shaw L.J., Slomka P.J., Berman D.S., "Pericardial fat burden on ECG-gated noncontrast CT in asymptomatic patients who subsequently experience adverse cardiovascular events on 4-year follow-up: A case-control study," *Journal of Am Coll Cardiol Cardiovascular Imaging*, pp. 352-360, 2010.
- [5] A.A. Mahabadi, M.H. Berg, N. Lehmann, H. Kalsch, M. Bauer, K. Kara, N. Dragano, S. Moebus, K. H. Jockel, R. Erbelet al., "Association of epicardial fat with cardiovascular risk factors and incident myocardial infarction in the general population: the Heinz Nixdorf Recall Study," (in eng), *J Am Coll Cardiol*, Journal Article Research Support, Non-U.S. Gov't vol. 61, no. 13, pp. 1388-95, Apr 2 2013.
- [6] B. Tamarappoo, D. Dey, H. Shmilovich, R. Nakazato, H. Gransar, V. Y. Cheng, J. D. Friedman, S. W. Hayes, L. E. Thomson, P. J. Slomka et al., "Increased pericardial fat volume measured from noncontrast CT predicts myocardial ischemia by SPECT," (in eng), *JACC Cardiovasc Imaging*, vol. 3, no. 11, pp. 1104-12, Nov 2010.
- [7] A. A. Mahabadi, J. M. Massaro, G. A. Rosito, D. Levy, J. M. Murabito, P. A. Wolf, C. J. O'Donnell, C. S. Fox, and U. Hoffmann, "Association of pericardial fat, intrathoracic fat, and visceral abdominal fat with cardiovascular disease burden: the Framingham Heart Study," (in eng), *Eur Heart J*, Journal Article vol. 30, no. 7, pp. 850-6, Apr 2009.
- [8] R.M. Abazid, O.A. Smettei, M.O. Kattea, S. Sayed, H. Saqqah, A. M. Widyan, and M. P. Opolski, "Relation Between Epicardial Fat and Subclinical Atherosclerosis in Asymptomatic Individuals," *Journal of Thoracic Imaging*, 2017.
- [9] R. Shahzad, D. Bos, C. Metz, A. Rossi, H. Kirişli, A. van der Lugt, S. Klein, J. Witteman, P. de Feyter, and W. Niessen, "Automatic quantification of epicardial fat volume on non-enhanced cardiac CT scans using a multi-atlas segmentation approach," *Medical physics*, vol. 40, no. 9, 2013.
- [10] A. Krizhevsky, I. Sutskever, and G. E. Hinton, "Imagenet classification with deep convolutional neural networks," in *Advances in neural information processing systems*, 2012, pp. 1097-1105.
- [11] O. Russakovsky, J. Deng, H. Su, J. Krause, S. Satheesh, S. Ma, Z. Huang, A. Karpathy, A. Khosla, and M. Bernstein, "Imagenet large scale visual recognition challenge," *International Journal of Computer Vision*, vol. 115, no. 3, pp. 211-252, 2015.
- [12] Y. LeCun, B. Boser, J. Denker, D. Henderson, R. Howard, W. Hubbard, and L. Jackel, "Handwritten digit recognition with a back-propagation network," in *Neural Information Processing Systems (NIPS)*, 1989.
- [13] K. Drukker, B. Q. Huynh, M. L. Giger, S. Malkov, J. I. A. Avila, B. Fan, B. Joe, K. Kerlikowske, J. S. Drukeinis, and L. Kazemi, "Deep learning and three-compartment breast imaging in breast cancer diagnosis," in *SPIE Medical Imaging*, 2017, pp. 101341F-101341F-6: International Society for Optics and Photonics.
- [14] B. Sahiner, C. Heang-Ping, N. Petrick, W. Datong, M. A. Helvie, D. D. Adler, and M. M. Goodsitt, "Classification of mass and normal breast tissue: a convolution neural network classifier with spatial domain and texture images," *IEEE*

Transactions on Medical Imaging, vol. 15, no. 5, pp. 598-610, 1996.
[15] S. Pereira, A. Pinto, V. Alves, and C. A. Silva, "Brain

tumor segmentation using convolutional neural networks in MRI images," *IEEE transactions on medical imaging*, vol. 35, no. 5, pp. 1240-1251, 2016